DOI: 10.1093/brain/awg138 Advanced Access publication April 8, 2003 *Brain* (2003), **126,** 1300–1318

Grey and white matter flumazenil binding in neocortical epilepsy with normal MRI. A PET study of 44 patients

Alexander Hammers,[1,2] Matthias J. Koepp,[1,2] Mark P. Richardson,[1,2] René Hurlemann,[2] David J. Brooks[1] and John S. Duncan[2]

[1]*MRC Clinical Sciences Centre and Division of Neuroscience, Faculty of Medicine, Imperial College London, Hammersmith Hospital, and* [2]*National Society for Epilepsy MRI Unit, Chalfont St Peter, and Department of Clinical and Experimental Epilepsy, Institute of Neurology, Queen Square, London, UK*

Correspondence to: Professor John S. Duncan, MA, DM, FRCP, Department of Clinical and Experimental Epilepsy, Institute of Neurology, 33 Queen Square, London WC1N 3BG, UK
E-mail: j.duncan@ion.ucl.ac.uk

Summary

In 20–30% of potential surgical candidates with refractory focal epilepsy, standard MRI does not identify the cause. γ-Aminobutyric acid (GABA) is the principal inhibitory neurotransmitter in the brain. [^{11}C]Flumazenil (FMZ) PET images most subtypes of $GABA_A$ receptors, present on most neurons. We investigated [^{11}C]FMZ binding in grey and white matter in 16 normal controls and in 44 patients with refractory neocortical focal epilepsy and normal optimal MRI. Fourteen patients had unilateral frontal lobe epilepsy, five occipital lobe epilepsy (OLE), six parietal lobe epilepsy (PLE) and 19 neocortical epilepsy that was not clearly lobar. Parametric images of FMZ volume of distribution (FMZ-V_d) were computed. Statistical parametric mapping (SPM99) with explicit masking, including the white matter, was used to analyse individual patients and groups. Thirty-three of the 44 patients showed focal abnormal FMZ-V_d; increases in 16, decreases in eight, and both increases and decreases in nine. In seven patients, the increases in FMZ binding were periventricular, in locations normally seen in periventricular nodular heterotopia on MRI. There were frontal and parietal increases in FMZ binding in grey and white matter in the PLE group and decreases in the cingulate gyrus in the OLE group. FMZ binding increases, particularly periventricular increases, were a prominent feature of MRI-negative focal epilepsies and may represent neuronal migration disturbances.

Keywords: SPM99; localization-related epilepsy; frontal lobe epilepsy; parietal lobe epilepsy; occipital lobe epilepsy

Abbreviations: FLE = frontal lobe epilepsy; FMZ = flumazenil; FOV = field of view; FWHM = full-width half-maximum; GABA = γ-aminobutyric acid; GM = grey matter; HS = hippocampal sclerosis; MCD = malformation of cortical development; MNI = Montreal Neurological Institute; NeuN = neuronal nuclear antigen; OLE = occipital lobe epilepsy; PLE = parietal lobe epilepsy; ROI = region of interest; SPM = statistical parametric mapping; TLE = temporal lobe epilepsy; TLWM = temporal lobe white matter; V_d = volume of distribution; WM = white matter

Introduction

In patients with partial seizures whose seizures have not been suppressed by optimal doses of two standard antiepileptic drugs, the chance of becoming seizure free with medication is <5% (Kwan and Brodie, 2000). In patients with medically refractory partial seizures, surgery offers the possibility of a cure if the epileptic focus can be defined. Advances in MRI have allowed the identification of structural abnormalities that are presumed to be the seizure focus in 70–80% of cases (Duncan, 1997). The remaining 20–30% of cases in whom no lesion is identified by high quality MRI present a particular challenge to epilepsy surgery centres. Surgery has a less favourable outcome when the presumed epileptogenic region is removed in the absence of identifiable pathology on imaging or the resected specimen (Jack *et al*., 1992; Berkovic *et al*., 1995). MRI may be normal even when

histopathological examination of resected specimens detects focal cortical dysplasia, hippocampal sclerosis (HS) or other pathologies (Chugani *et al*., 1990; Kuzniecky *et al*., 1991; Desbiens *et al*., 1993; Van Paesschen *et al*., 1997).

γ-Aminobutyric acid (GABA) is the principal inhibitory neurotransmitter in the brain, acting at the $GABA_A$ receptor complex. Flumazenil (FMZ) is a specific, reversibly bound high affinity neutral antagonist at the benzodiazepine-binding site of $GABA_A$ receptors (Olsen *et al*., 1990) containing α-subunits 1, 2, 3 or 5, which are expressed by most neurons. [^{11}C] FMZ PET provides a useful *in vivo* marker of $GABA_A$ receptor binding (Maziere *et al*., 1984).

Epileptogenic foci generally have been reported to exhibit decreased [^{11}C]FMZ binding (Savic *et al*., 1988, 1993, 1995; Henry *et al*., 1993; Szelies *et al*., 1996; Koepp *et al*., 1997*a*, 2000; Richardson *et al*., 1998*b*; Ryvlin *et al*., 1998; Muzik *et al*., 2000). Some studies, however, have found localized increases in the number or affinity of $GABA_A$ receptors (Hand *et al*., 1997; Brooks-Kayal *et al*., 1998), and areas of increased [^{11}C]FMZ volume of distibution (V_d) may also mark the epileptogenic zone in some forms of focal epilepsy. *In vivo*, we have shown previously that malformations of cortical development (MCDs) frequently are associated with increases of FMZ-V_d (Richardson *et al*., 1996, 1997), whereas no increases of FMZ binding were seen in acquired lesions (Richardson *et al*., 1998*b*).

MCDs are increasingly recognized as underlying medically intractable epilepsy (Kuzniecky and Jackson, 1997). Microdysgenesis, a minimal form of MCD, is by definition not detectable on current MRI and is usually defined as an increased density of heterotopic neurons in the stratum moleculare or the white matter (WM) (Raymond *et al*., 1995). Some WM neurons are found in healthy controls, and the distinction is quantitative (Hardiman *et al*., 1988; Emery *et al*., 1997; Kasper *et al*., 1999; Thom *et al*., 2001), with very marked regional variation (Rojiani *et al*., 1996). At the other end of the spectrum, when a critical density and extent are reached, heterotopic neurons can be identified macroscopically or by MRI as heterotopic grey matter (GM) (Raymond *et al*., 1995).

We recently demonstrated a strong and highly significant correlation between *in vivo* temporal lobe white matter (TLWM) FMZ binding and WM neuron number, determined semi-quantitatively *ex vivo*, in patients with HS who underwent anterior temporal lobe resection (Hammers *et al*., 2001*a*) and similar increases in temporal lobe epilepsy (TLE) with normal MRI (Hammers *et al*., 2002*b*).

The aims of the current study were to test the hypotheses that: (i) FMZ PET may reveal focal abnormalities in patients with medically refractory focal neocortical epilepsies and normal, high resolution MRI; (ii) in this patient group, there are abnormalities of FMZ binding in WM, that are a marker of heterotopic WM neurons; and (iii) there may be common abnormalities detected in group comparisons of homogenous patient populations.

Material and methods

Patients and controls

We studied 44 patients (18 women) with medically refractory neocortical focal epilepsy. They had either unilateral frontal lobe epilepsy (FLE; $n = 14$; numbered F1–F14), parietal lobe epilepsy (PLE; $n = 6$; numbered P1–P6) or occipital lobe epilepsy (OLE; $n = 5$; numbered O1–O5). The remainder ($n = 19$; numbered X1–X19) were classified as neocortical epilepsies without clear lobar origin. Diagnosis was based on seizure semiology, prolonged interictal EEG in all, and ictal video-EEG findings in 31 out of 44 patients (Table 1). Patients were recruited from the epilepsy clinics of the National Hospital for Neurology and Neurosurgery, Queen Square, London, UK, and the National Society for Epilepsy, Chalfont St Peter, UK. All patients had normal optimal MRI and were potential candidates for surgical treatment at the time of inclusion in the study.

The median age at onset of habitual seizures was 10 years (range: 1–34), the median duration of epilepsy before the PET examination was 17 years (range: 4–58 years), and the median age at PET examination was 26 years (range: 18–61 years). None had a history of prolonged febrile convulsions.

Patients had a median of 96 complex partial seizures per year (range: 2–1100). Their antiepileptic medication was carbamazepine (32 patients), lamotrigine (13), gabapentin (eight), phenytoin (eight), sodium valproate (seven), topiramate (six), remacemide (two), and one each was treated with vigabatrin, oxcarbazepine and tiagabine. One patient was treated with a vagal nerve stimulator. Two were on no medication, 12 on monotherapy, 26 on two antiepileptic drugs and five on three drugs. Patients who were treated with benzodiazepines or barbiturates within 2 months of the PET examination were not included in the study as these drugs could possibly interfere with [^{11}C]FMZ binding.

Sixteen healthy volunteers (four women) were studied for comparison. The median age at examination was 46 years (range: 26–61). They had no history of neurological or psychiatric disorder and were on no medication.

Individuals did not consume alcohol within the 48 h preceding PET.

Written informed consent was obtained in all cases according to the Declaration of Helsinki. The approvals of the Joint Ethics Committee of The Institute of Neurology and The National Hospital for Neurology and Neurosurgery, the Ethics Committee, Imperial College, Hammersmith Hospital and of the UK Administration of Radiation Substances Advisory Committee (ARSAC) were obtained.

Clinical data for all 44 patients are shown in Table 1. So far, one patient has undergone resective epilepsy surgery (patient F11).

PET

We used the same acquisition technique as described previously (Hammers *et al*., 2002*a*). PET scans were

Table 1 *Clinical, EEG and imaging data in 44 patients with refractory partial epilepsy and normal MRI*

Pat. no.	Age (years) /sex	Onset/ duration (years)	Seizures/ year	Interval from last CPS→ PET	Treatment	Seizures	EEG (inter-ictal)	EEG (ictal)	Probable focus localization	FMZ PET: increases	FMZ PET: decreases	FMZ PET: PV WM increases >2.5 SD
F1	36/F	7/29	360	16 h	PHT	L sensorimotor SPS; CPS with arm dystonia; 2° GTCS	Runs of bilateral anterior dominant sharp and slow. Some sharp waves in R fronto-temporal region	Generalized attenuation only	R FL	L inferior frontal G	NS	Bilateral central/ posterior
F2	22/M	1/21	36	42 days	CBZ/PHT/VPA	Head turns to L; L arm dystonia, taps R hand	Continuous R mid-front slow; occ sharp activity in same area.	none	R FL	NS	L lateral middle frontal G, L medial precuneus, L medial OL WM, L posterior cingulate G, ext. to R, L precentral G	None
F3	21/M	4/17	480	16 h	CBZ/GBP	Head turns to R; R limb jerking; second pattern arm dystonia and facial contortion	L central sylvian high amplitude fast and spike activity	L central sylvian high amplitude fast and spike activity at seizure onset	L FL	NS	NS	L central + anterior
F4	18/F	7/11	24	21 days	LTG	R arm dystonic and rising; head turns to R; 2° GTCS	Bilateral anteriorly predominant non-specific abnormalities; more localized sharp waves in L frontal region	None	L FL	L central PV ext. to L anterior PV, L superior PL, L paracentral lobule, R anterior PV ext. to central PV, L precentral G, R posterior PV	R FL middle frontal G, R lateral inferior TL widespread, L inferior posterior TL, L middle occipital G	Bilateral widespread with central and anterior emphasis
F5	26/M	5/21	480	2 h	CBZ/PHT REM	Dystonic asymmetrical arm posturing, head looks down	R frontal slow and sharp	R frontal fast activity	R FL	R superior frontal G, L FL orbitofrontal gyri, L central/posterior PV, L middle temporal G (2 clusters)	R superior temporal G, R occipitotemporal WM, L inferior frontal G, R middle frontal G, bilateral medial FL	Bilateral posterior and L anterior/central
F6	28/F	11/17	48	28 days	LTG	CPS with head turning to L; wanders around and may run; 2° GTCS	Low amplitude slow and sharp R fronto-temp	No significant change with self-reported attack	R FL	NS	NS	Bilateral posterior
F7	24/F	6/18	144	3 days	CBZ/GBP	Tingling in mouth, R arm posturing, evolving to 2° GTCS	L fronto-temporal spikes	Generalized attenuation, then rhythmic discharge L fronto-central	L FL	NS	NS	Bilateral posterior, L central, R anterior
F8	18/M	11/7	96	14 days	CBZ/PHT	Frequent nocturnal; head turns to L, L arm rises	L front frequent spikes	None	L FL	L FL precentral G>L PL postcentral G, L central PV WM	R medial PL, R middle frontal G	L central> anterior> posterior

Table 1 *Continued*

Pat. no.	Age (years) /sex	Onset/ duration (years)	Seizures/ year	Interval from last CPS→ PET	Treatment	Seizures	EEG (inter-ictal)	EEG (ictal)	Probable focus localization	FMZ PET: increases	FMZ PET: decreases	FMZ PET: PV WM increases >2.5 SD
F9	24/F	6/18	360	1.5 days	CBZ/GBP	L face contorts with L limb movements		Irregular widespread rhythmical activity	R FL	R postcentral >precentral G WM	NS	Bilateral central
F10	30/M	6/24	30	28 days	LTG/VPA	Loss of awareness, stretches out, staring ahead, purposeful movements of arms, L leg kicking out	Some delta R>L	Irregular slow and sharp waves at FP2	R FL	R superior and middle frontal gyrus, widespread, ext. to L, R precentral G (2 clusters), R middle frontal G WM> GM, L middle precentral G, L anterior cingulate G	NS	R anterior and bilateral posterior
F11	33/F	23/10	84	7 days	CBZ/ TPM	Loss of awareness, leg automatisms	R fronto-temporal slow; intracranial recordings: higher amplitude irregular slow R lateral frontal strip, intermittent R central slow. propagated abnormalities L frontal strip/rhythmic R central sharp	Surface recordings: bifrontal slow, R>L. Intracranial recordings: R orbito-frontal spike-wave just before clinical onset.	R FL (inferior orbito-frontal)	L FL, ext. to R FL, widespread anteriorly, incl. WM, L inferior parietal lobe, L middle frontal G, R orbitofrontal WM, R medial frontal G, anterior to precentral G, L anterior insula/inferior frontal G, bilateral medial FL	None	R posterior, L anterior
F12	26/M	22/4	72	14 days	CBZ	CPS: loss of awareness, fiddling with clothes, standing up/falls, confused	Epileptiform activity bifrontal L>R or widespread over L hemisphere in sleep	None	L FL	L middle frontal G WM/GM	NS	R posterior
F13	37/M	30/7	96	2 days	None	Mostly nocturnal; stiffening or thrashing of all 4 limbs	some slow fronto-temporal regions L>>R	L frontal slow, maximum F3/C3	L FL	NS	NS	R central
F14	23/M	4/19	540	22 h	CBZ/LTG/ TPM	CPS with straightening, turning to L, may giggle; tonic seizures; 2º GTCS with R sided Todd's paresis	Frequent bifronto-temporal spike wave activity, more marked over L.	bilateral attenuation, then semirhythmic 5Hz activity L anterior area	L FL	R FL middle frontal G> superior and medial G GM/WM	NS	R anterior

Table 1 *Continued*

Pat. no.	Age (years) /sex	Onset/ duration (years)	Seizures/ year	Interval from last CPS→ PET	Treatment	Seizures	EEG (inter-ictal)	EEG (ictal)	Probable focus localization	FMZ PET: increases	FMZ PET: decreases	FMZ PET: PV WM increases >2.5 SD
P1	37/M	4/33	120	14 days	OXC/PHT	L leg sensory SPS evolving to 2° GTCS	Theta more marked R hemisphere	High voltage polyspike/wave, no clear lat	R PL	NS	L OL WM, R OL WM	None
P2	26/M	6/20	52	2 days	CBZ/ GBP	Numbness or pain R arm, sometimes spreading to R leg, aphasia	Irregular sharp theta bursts with L temporal emphasis; sharp wave trains prominently over vertex and mid-parietal areas	Sharp and slow waves over the central region, more pronounced over the L	L PL	R middle frontal G, L superior frontal G, L middle frontal G, L precentral> postcentral G, L FL WM superior and middle frontal G	NS	R posterior
P3	55/M	7/48	168	60 days	CBZ/PHT	Sensation of numbness and twitchiness R arm	Non-specific bitemporoparietal abnormalities	None	L PL	L FL anterior superior frontal G L frontal operculum, R superior frontal G, GM/WM, L middle frontal gyrus GM/WM	NS	L posterior
P4	19/F	1/18	21	120 days	CBZ	Paraesthesia and numbness L arm, then jerking L arm	L fronto-centro-temporal sharply formed waves; some theta/delta bilaterally	None	R PL	NS	L middle frontal G	None
P5	27/M	5/22	1095 (SPS)	12 h	VPA	SPS: throbbing feeling R arm, stutters	Small polysharp waves bilaterally but especially over L temporo-parietal region	Possible attenuation L>R, no clear lateralizing or localizing features	L PL	L postcentral G>L precentral G, L middle frontal G, R superior PL	NS	R central
P6	34/F	25/9	100	7 days	CBZ/ GBP/ LTG	L sensorimotor SPS, may evolve to 2° GTCS	R sided continuous slow activity + infrequent epileptiform discharges, max fronto-central or posterior temporal/occipital	Rhythmic discharge over R hemisphere	R PL	L inferior PL GM/WM, R PLWM ext. to posterior lateral ventricle	R orbitofrontal gyri	R>L posterior, bilateral central
O1	25/M	8/17	24	7 days	CBZ/ GBP	SPS with R visual field phenomena, may evolve to 2° GTCS, R>L	Spikes L posterotemporo-occipital region, maximum T5/O1.	L post temp/occ repetitive sharp waves	L OL	NS	L medial OL extending to R medial OL (large cluster)	R posterior, L central, R anterior
O2	32/M	10/22	7 (SPS)	14 days	CBZ/ LTG	SPS with bil flashing lights, coloured shapes and formed images	Fairly frequent bursts of spikes or sharp waves bilateral posteriorly	None	OL, ? lateralization	NS	NS	R posterior

Table 1 *Continued*

Pat. no.	Age (years) /sex	Onset/ duration (years)	Seizures/ year	Interval from last CPS→ PET	Treatment	Seizures	EEG (inter-ictal)	EEG (ictal)	Probable focus localization	FMZ PET: increases	FMZ PET: decreases	FMZ PET: PV WM increases >2.5 SD
O3	33/F	16/17	12 (SPS)	61 days	CBZ	SPS with feeling of brightness and fear, head and eyes to L, blinking eyelids	Bursts of theta waves with no consistent side emphasis	None	OL, ?lateralization	L inferior PL, R middle frontal G	NS	R central
O4	39/M	34/5	3 (SPS)	105 days	CLB prn	Blurred vision, eyelid blinking, sweating forehead	Normal	None	OL, ?lateralization	NS	NS	L central, R posterior
O5	26/F	10/16	2	90d	TPM	Distorted vision L upper quadrant or flashing lights L hemifield, decreased awareness	Intermittent theta, sometimes of sharp morphology, in the temporal regions	None	R OL	NS	L precentral G	R posterior
X1	23/M	6/17	480	4 h	CBZ/ LTG	R sensory SPS; CPS with L arm automatisms; 2° GTCS	Indep L and R post temp spikes	Gen atten; late R temp theta in one attack	L and R post temp	NS	Bilateral OL	L central and temporal
X2	26/M	15/11	144	7 days	CBZ/ PHT	Frequent noct jerking arms and legs. CPS with no clear lateralization	Ant dominant runs of sharp delta	Diffuse high voltage sharp, then diffuse slow	FL, ?lateralization	L central PV	R middle frontal G, L middle temporal G, R medial PL, L medial frontal G, R anterior insula/FL WM, R orbitofrontal WM, R medial frontal G	L central + anterior
X3	18/F	8/10	36	1 day	CBZ/ REM	SPS (auditory phenomena); may progress to CPS: head turning to L. Further pattern with R arm dystonia and head turning to R	Bifrontal sharpened slow wave transients; independent sharp/slow wave in fronto-temporal regions; runs of semi-rhythmic 3–5Hz independently over both hemispheres (anterior predominance); occasional independent bitemporal spikes	First pattern: R ant temp theta. Second pattern: L post temp sharp	R ant temp and L post temp	L FL WM lateral of head of caudate nucleus	R middle and inferior temporal G, R middle frontal G (2 clusters), R posterior PL	L central and anterior, R central

Table 1 *Continued*

Pat. no.	Age (years) /sex	Onset/ duration (years)	Seizures/ year	Interval from last CPS→ PET	Treatment	Seizures	EEG (inter-ictal)	EEG (ictal)	Probable focus localization	FMZ PET: increases	FMZ PET: decreases	FMZ PET: PV WM increases >2.5 SD
X4	40/M	27/13	48	2d	CBZ/ LTG	CPS: stands, claps hands, rocks back and forward if sitting	Frequent high amplitude sharp waves over both frontal regions	None	FL, ?lateralization	L superior PL, R precentral G, L PL WM ext. to bilat. central PV, L FL WM between caudate nucleus and cortex, R superior PL	NS	L central>anterior, R central> anterior>posterior
X5	47/M	10/37	72	2 days	CBZ/ GBP	CPS with repetitive facial movements, head turning to L; may evolve to 2° GTCS	Spikes during sleep, max. at F8 and R superficial sphenoidal. Rare similar independent runs on L	Fast activity R posterior temporal/occipital (T6/O2)	R post temp	R superior PL	R OL/PL WM, R middle temporal G, R middle frontal G (2 clusters)	R central/ posterior
X6	39/M	9/30	192	12 h	CBZ/ LTG	Mainly nocturnal CPS: arms held rigidly straight in front; may evolve to 2° GTCS	Bil ant slow	Bilateral central rhythmic activity and distorted spikes and sharp. No clear lat.	FL, ?lateralization	NS	NS	R posterior and anterior
X7	24/M	19/5	32	90 days	CBZ	SPS: numbness in mouth, L side of face pulled upwards, drooling; L wrist flexing; may evolve to 2° GTCS	Frequent sharp waves/spike discharges in R centro-temporal region	Artefact; possible slow wave rhythmic discharge R hemisphere	R centrotemp	NS	NS	Bilateral central
X8	20/F	11/9	10	7 days	CBZ/ VPA	Speech disturbance, stares, may put R hand on chest	Predominantly bifrontal sharp waves	L>R anterior rhythmic discharge + spikes	Neocortical, L hemisphere	NS	R medial posterior PL, R TL WM	L central
X9	42/M	33/9	264	1 day	GVG/ PHT	Mostly nocturnal CPS: walking around or falls, leg>arm movements	Predom. L mid-ant temporal spikes + R temp indep discharges	7–10 s after clin onset: semi-rhythmic slow R frontal region, wide field, no clear localization	Neocortical, ?localization	R medial orbitofrontal gyri, R FL WM/GM between superior and medial frontal G	NS	None
X10	18/F	7/11	12	75 days	LTG/ VPA	Head→L, stiffening and posturing of the limbs, nocturnal 2° GTCS	Some non-specific changes in posterior temporal areas	Semi-rhythmic 7–8 Hz discharge, maximum R centrotemporal-parietal	Neocortical, R hemisphere	L FL WM under inferior frontal G	R medial posterior PL	Bilateral central
X11	19/F	13/6	48	7 days	LTG/ TPM	L hand postured, head and eyes to R	Spikes and sharp/slow wave transients in R posterior temporal region (sleep)	Semi-rhythmic slow activity over the R, maximum T6	R posterior temporal/ occipital	NS	NS	None

Table 1 *Continued*

Pat. no.	Age (years) /sex	Onset/ duration (years)	Seizures/ year	Interval from last CPS→ PET	Treatment	Seizures	EEG (inter-ictal)	EEG (ictal)	Probable focus localization	FMZ PET: increases	FMZ PET: decreases	FMZ PET: PV WM increases >2.5 SD
X12	59/F	33/26	1000	1 day	GBP/ VPA	Starts with mvt R hand, then irregular thrashing of all limbs	Small amplitude sharp waves in both anterior quadrants	Movement artefacts, no clear EEG change	FLE, ?lateralization	R orbitofrontal gyri, L>R medial FL and frontal poles widespread, R superior frontal G	L medial inferior postcentral gyrus (Fig. 3)	Bilateral posterior and L anterior
X13	38/F	10/28	220	5 days	CBZ/ TPM	Limb automatisms, vocalization, head turning	Normal	Bilateral (frontal) rhythmic changes without clear localization	FLE, ?lateralization	L FL WM/GM between medial and middle frontal G, R FL WM/GM between medial and middle frontal G	NS	None
X14	25/F	17/8	1100	2.5 h	CBZ/ LTG	SPS, CPS: loss of awareness, tearing at clothing, fiddling, confused	Widespread independent epileptiform discharges over both temp. regions, sometimes more ant	R fronto-centro-temporal	Neocortical, R hemisphere	NS	L medial PL and medial posterior TL	Bilateral posterior + bilateral central
X15	26/F	3/22	250	4 days	CBZ/ TGB/ TPM	CPS: crying out, fiddling, coughing	Predominantly anterior bilateral epileptiform activity, sometimes L sided emphasis	Bilateral, start in L hemisphere	L hemisphere	NS	NS	R anterior and posterior, L central
X16	37/M	24/13	300	1 day	CBZ/ VPA	Blank stare, head jerking	independent mid-temp spikes and slow	Bilateral, initially R fronto-temp-central rhythmic discharge	R hemisphere	L anterior superior frontal gyrus	NS	L central and bilateral anterior
X17	24/M	13/11	170	2 days	CBZ/ LTG	Eyes and head to R, R arm and leg extended and jerking, bimanual automatisms	Bifrontal/ generalized semi-rhythmic sharp and slow activity, left sided predominance	Generalized attenuation followed by generalized, anterior predominant, semi-rhythmic slow	Neocortical, ?L FL	NS	NS	R posterior, bilateral central
X18	18/M	11/7	150	4 days	CBZ/ VNS	No warning, loss of awareness, derealization, abnormal space and voice perception, R arm>leg may twitch	Bilateral non-specific abnormalities, bilateral sharp waves/spikes posteriorly, maximum R centro-temporal	None	Neocortical, ? localization	L anterior middle frontal G	NS	Bilateral central

Table 1 *Continued*

Pat. no.	Age (years) /sex	Onset/ duration (years)	Seizures/ year	Interval from last CPS→ PET	Treatment	Seizures	EEG (inter-ictal)	EEG (ictal)	Probable focus localization	FMZ PET: increases	FMZ PET: decreases	FMZ PET: PV WM increases >2.5 SD
X19	61/M	3/58	12	120 days	CBZ	Complete amaurosis, head thrown back	Isolated epileptiform discharges in parietal and central regions bilaterally, R>L; bilateral spike–wave discharge after hyperventilation	None	Neocortical, ?localization	R medial orbitofrontal gyri + frontal pole, L middle frontal G, L lateral PL, R medial PL extending to R central PV, L anterior OL/posterior PL, L inferior occipital G, L postcentral G	NS	Bilateral central and posterior, L central

R = right; L = left; CPS = complex partial seizure(s); 2° GTCS = secondarily generalized tonic–clonic seizures; CBZ = carbamazepine; CLB = clobazam; G = gyrus; GBP = gabapentin; GVG = vigabatrin; h = hours; LTG = lamotrigine; mvt = movement; OXC = oxcarbazepine; PHT = phenytoin; REM = remacemide; SPS = simple partial seizures; TPM = topiramate; VNS = vagus nerve stimulator; VPA = valproic acid; prn = pro re nata; FL = frontal lobe; OL = occipital lobe; PL = parietal lobe; TL = temporal lobe; PV = periventricular. Increases and decreases of FMZ-V_d, compared with the control group are sorted by height of *Z* scores.

performed on a 953B Siemens/CTI PET camera in 3D mode with the septa retracted, giving a reconstructed image resolution of ~4.8 × 4.8 × 5.2 mm in air in the centre of the scanner field of view (FOV) at full-width half-maximum (FWHM) for 31 simultaneously acquired planes (Bailey, 1992). Reconstructed voxel sizes were 2.09 × 2.09 × 3.42 mm. Scans were performed with transaxial planes parallel to a horizontal plane through the anterior and posterior commissures. A transmission scan using three rotating $^{68}Ga/^{68}Ge$-rotatory line sources was performed to enable attenuation correction of the emission scans. An eight-channel EEG was recorded during the PET studies to ensure that the scans were interictal. High specific activity [^{11}C]FMZ tracer (370 MBq) (Maziere *et al*., 1984) was injected intravenously. Arterial blood was sampled continuously to determine a metabolite-corrected plasma input function (Lammertsma *et al*., 1993). A dynamic 3D series, consisting of 20 frames over 90 min, was acquired for the brain volume. A convolution subtraction scatter correction was used (Bailey, 1992) and axial-scaling with the inverse of the scanner's axial profile applied to obtain uniform efficiency throughout the FOV (Grootoonk, 1995). To minimize any movement artefact during the scan, the 20 time frames of the dynamic image were realigned with one another by an automated 'least-squares' technique (Friston *et al*., 1995*a*). Parametric images of [^{11}C]FMZ-V_d, reflecting binding to $GABA_A$ receptors at the voxel level (Koeppe *et al*., 1991), were produced from the brain uptake and metabolite-corrected arterial plasma input functions using spectral analysis (Cunningham and Jones, 1993) with correction for blood volume.

MRI

MRIs were obtained using a gradient echo protocol on a 1 T Picker scanner (Picker, Cleveland, OH, USA) which generated 128 contiguous 1.3 mm thick sagittal images [matrix 256 × 256 voxels, voxel sizes 1 × 1 × 1.3 mm, repetition time (TR) 35 ms; echo time (TE) 6 ms; flip angle 35°]. These high resolution volume acquisition MRI scans were co-registered to the parametric images of [^{11}C]FMZ binding. In addition, all patients had studies with a 1.5 T General Electric Signa Echospeed scanner (Milwaukee, USA). Sequences included coronal oblique proton density and T_2-weighted studies, a coronal oblique fast fluid attenuation inversion recovery (Fast FLAIR) sequence and a coronal T_1-weighted 3D volume [inversion recovery prepared fast spoiled gradient recall (General Electric), TE/TR/number of excitations (NEX) 4.2 (fat and water in phase)/15.5/1, time of inversion (TI) 450, flip angle 20°, 124 slices of 1.5 mm thickness, FOV 18 × 24 cm with a 192 × 256 matrix], covering the whole brain with voxel sizes of 0.9375 × 0.9375 × 1.5 mm.

All MRIs were reported to be normal on inspection by two experienced neuroradiologists.

PET image analysis

[^{11}C]FMZ-V_d images were analysed within the framework of statistical parametric mapping (SPM99, Wellcome Department of Cognitive Neurology, London, UK) implemented in Matlab version 5 (Mathworks Inc., Sherborn, MA, USA), using a cluster of Sun Ultra 10 workstations (Sun Microsystems, Mountain View, CA, USA). The images were normalized volumetrically to a symmetrical reference FMZ-V_d template created in our unit that occupies the same Montreal Neurological Institute (MNI) standard space as the SPM99 MRI templates. These are based on an average of 152 MRIs supplied by the MNI that have been linearly matched to the brain in the atlas of Talairach and Tournoux (1988). The normalization procedure involved a linear 3D transformation and used a set of smooth basis functions that allow for normalization at a finer anatomical scale (Ashburner and Friston, 1999). Images were smoothed using a 12 × 12 × 12 mm (FWHM) isotropic Gaussian kernel as a final preprocessing step. This spatial filter accommodates interindividual anatomical variability and improves the sensitivity of the statistical analysis (Friston *et al*., 1991). Each patient's MRI scan was co-registered with their FMZ-V_d image (Woods *et al*., 1993; Ashburner and Friston, 1997) and then transformed into standard space using the transformation matrix derived from the spatial normalization of that individual's FMZ-V_d image.

Statistical analysis

Significant differences in FMZ binding between patients and control subjects were localized by applying the general linear model to each and every voxel of the normalized and smoothed images (Friston *et al*., 1995*b*). Statistical parametric maps are 3D projections of statistical functions that are used to characterize significant regional differences in imaging data. We have described the use of SPM in [^{11}C]FMZ PET studies of patients with unilateral hippocampal sclerosis (Koepp *et al*., 1996; Hammers *et al*., 2001*a*), in patients with MCDs (Richardson *et al*., 1997) and in patients with TLE and normal MRI (Koepp *et al*., 2000; Hammers *et al*., 2002*b*). SPM99 combines the general linear model to create the statistical map, and random field theory to make statistical inferences about regional effects (Friston *et al*., 1995*b*; Worsley *et al*., 1996).

Each control was compared against the remaining 15 controls, using the same design matrices as for the patients, with the design matrix designating global cerebral FMZ-V_d differences and age as nuisance covariates (Friston *et al*., 1990). The same type of analysis was performed for the *post hoc* analysis of the magnitude of the difference of FMZ binding between patients and controls in the periventricular area (see below).

Individual patients were then compared with the 16 normal control subjects For the purposes of between-group statistical analyses, the [^{11}C]FMZ-V_d images of patients with unilateral lobar epilepsy were reversed before spatial manipulation so that the focus was on the same side in all patients. The data sets of patients with seizures arising from the side most frequently affected within each group were left unflipped so that the smallest possible number of data sets needed reversing.

Linear contrasts were used to test the hypotheses for specific focal effects. The resulting set of voxel values for each contrast constitutes an SPM of the t statistic SPM $\{t\}$. The SPM $\{t\}$ were thresholded at $P = 0.001$ uncorrected. The significance of foci of relative FMZ-V_d changes is estimated using random field theory, correcting for multiple comparisons using the number of independent resolution elements (resels) in the statistical image (Worsley *et al*., 1992, 1996). This examines the probability that the observed cluster of voxels could have occurred by chance, given its extent and peak height. The threshold chosen for the corrected cluster P values was $P < 0.05$. No extent thresholding was applied. This is referred to as 'conventional threshold' in the Results and Discussion.

Initial exploration of the data revealed significant periventricular increases in a localization typical for subependymal periventricular nodular heterotopia (Raymond *et al*., 1994; Dubeau *et al*., 1995) in a number of patients. In a *post hoc* analysis, therefore, we examined periventricular areas in all patients and controls with a mask encompassing ~5 mm of tissue around the ventricular system (Fig. 1) as obtained from segmentation of the MNI T_1 MRI template. We used the framework of SPM to search for effect sizes exceeding 2.5 SD of the control mean in a precisely defined search volume, as we were testing a specific hypothesis in a restricted area (Koepp *et al*., 2000; Hammers *et al*., 2001*a*, 2002*b*).

Age at onset of epilepsy, duration of epilepsy, frequency of seizures and interval between scan and last seizure were defined as covariates of interest and tested separately for their effect on FMZ-V_d. Age was included as a nuisance variable in the design matrix in all comparisons.

The aim was to localize abnormalities of FMZ-V_d in individual patients, compared with the control group, and between the control and patient groups, in both GM and WM. We therefore created an anatomical mask in template space, encompassing the GM in the cortex, the basal ganglia and the WM, to include all these areas in the statistical analysis (Fig. 1).

To exclude the possibility that the overall composition of the control group could influence results, we reanalysed one of the patients (F4) with periventricular increases of FMZ binding, substituting the current control group with a different one that has been used in a study of TLE (Hammers *et al*., 2002*b*). This second control group had been scanned in the same orientation as the current control group, but centred on the temporal lobe. Therefore, the vertex was not always included in the FOV, and it could not be used for this study. The periventricular areas, however, were present in the centre of the FOV in all cases, allowing the verification of the finding of periventricular increases of FMZ binding.

Fig. 1 Explicit mask in template space, incorporating neocortical and basal ganglia white matter (white); the periventricular mask is overlaid (grey).

In the largest homogenous group (unilateral FLE), with seven right-sided and seven left-sided cases, the group analysis was repeated after flipping the other half of data sets to ensure that the reversing and subsequent normalization to our symmetrical template had no, or only a minor, influence on the results. The same procedure was performed in the PLE group, with three patients having a right-sided and three a left-sided seizure focus.

To exclude the possibility that our findings were due to normalization artefacts, we performed a region of interest (ROI) analysis on the raw, unnormalized parametric V_d map of a patient who had shown periventricular increases of FMZ binding (patient X4). Circular ROIs sampling ~2000 mm^3 were placed on three adjacent slices in the appropriate periventricular areas in all 16 controls and the patient, and absolute FMZ-V_d values were measured directly.

Results

Controls

Comparing each individual control subject against the remaining 15 controls, one individual showed an increase of FMZ-V_d in the left anterior pallidum [$Z = 4.55$, k (number of voxels) = 407, $P < 0.001$] and another in the left parietal lobe ($Z = 4.14$, $k = 189$, $P = 0.027$). Given the chosen thresholds and the number of comparisons resulting from 16 controls $\times$ 2 contrasts, 1.6 positive results would be predicted by chance. Thus, our control group did not contain outliers, and we could verify our expected false-positive rate empirically. No control had any significant increases around the ventricles at the conventional threshold.

Comparing each individual control subject's periventricular region against the corresponding area in the remaining 15 at the lower threshold of $P < 0.01$ uncorrected for the *post hoc* analysis, five out of 16 showed increases within the periventricular mask.

There was a significant negative correlation between age and FMZ binding in the right middle and superior frontal lobe, the left precentral gyrus and the right parietal lobe, leading to the inclusion of age as a nuisance variable in all tests. There were no significant correlations with gender.

Unilateral frontal lobe epilepsy

Individual patients (see Table 1)

Four patients (F3, F6, F7 and F13) had no significant changes at conventional thresholds. Another four had single areas of increased FMZ binding (F1, F9, F12 and F14); two of these (in patients F9 and F12) were in the ipsilateral frontal lobe. Two more had multiple areas of increased FMZ-V_d (F10 and F11); in both, these included large areas of the ipsilateral frontal lobe. One patient (F2) had only areas of decreased FMZ binding; these were located in the contralateral hemisphere. Three patients had multiple areas of increased as well as multiple areas of decreased FMZ-V_d (F4, F5 and F8). In all three, increases included the ipsilateral frontal lobe, and represented the only increases in two of them (F4 and F8). All three had decreases outside the ipsilateral frontal lobe. Three patients (F4, F5 and F8) had clusters of increased FMZ binding around the ventricles at conventional thresholds. The periventricular locations at conventional thresholds were bilateral central, bilateral anterior and contralateral posterior in one (F4, Fig. 2), contralateral central and posterior in another (F5) and ipsilateral central in the third (F8).

The *post hoc* analysis revealed periventricular increases in 13 out of 14 patients, including the four in whom no abnormality had been found previously (see Table 1). The only patient who did not show any periventricular increases was the isolated case with areas of decreased FMZ-V_d but no areas of increased FMZ-V_d (F2). The periventricular increases in the *post hoc* analysis included, alone or in combination, the anterior horn in eight out of 13, central periventricular areas in seven out of 13 and the posterior horn in nine out of 13.

Group analysis

All 14 patients were included in the group analysis. Data sets of patients with right-sided foci were flipped to the left before normalization. There were no significant changes at conventional thresholds. In the *post hoc* analysis, ipsilateral frontal lobe WM increases were seen, extending to the ipsilateral central lateral ventricle.

Parietal lobe epilepsy

Individual patients (see Table 1)

All six patients had significant abnormalities at conventional thresholds. Three patients (P2, P3 and P5) had multiple areas with increased FMZ binding. These were bifrontal in all three and included the ipsilateral parietal lobe in two (P2 and P5). Two patients (P1 and P4) showed only areas of decreased FMZ-V_d. These were bilateral occipital in one (P1), and the other one (P4) had a single area of decrease in the frontal lobe contralateral to the presumed seizure focus. The remaining patient (P6) had biparietal increases as well as an area of significantly decreased FMZ-V_d in the ipsilateral orbitofrontal cortex. This patient also had periventricular increases

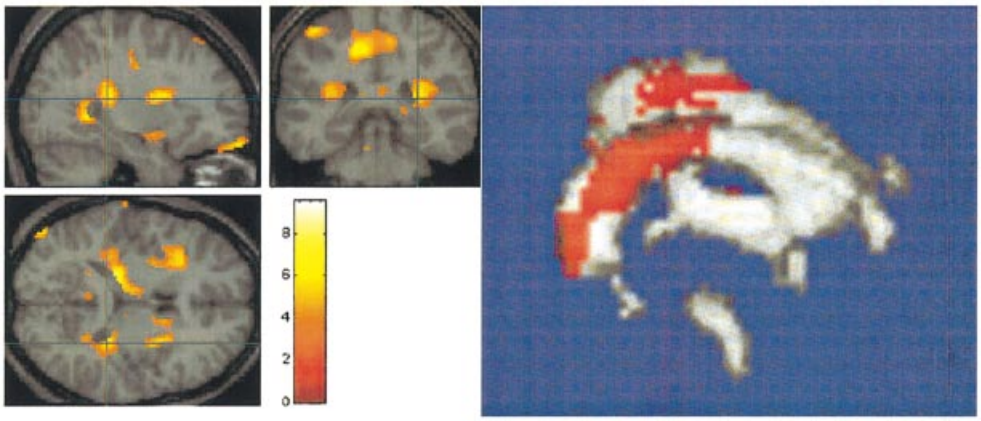

Fig. 2 Example of a patient (F4) with increased FMZ-V_d around the posterolateral ventricles bilaterally. Colour scale: *t* score (maximum $t = 8.52$, corresponding to $Z = 4.87$). Statistical results are overlaid onto the patient's co-registered MRI on the left of the figure; the right shows a 3D rendering of the statistical results (in red) overlaid onto the patient's ventricles (in white) to show their spatial relationship.

($Z = 4.37$, $k = 435$, $P = 0.001$) around the ipsilateral posterosuperior lateral ventricle. These were connected with the ipsilateral parietal increase.

The *post hoc* analysis revealed periventricular increases in four out of six patients (see Table 1); only the two patients with areas of decreased FMZ-V_d, but no areas of increased FMZ-V_d, failed to show any periventricular increases (P1 and P4). The periventricular increases in the *post hoc* analysis included, alone or in combination, the anterior horn in none, central periventricular areas in two out of four and the posterior horn in three out of four.

Group analysis

There were two significant clusters of FMZ-V_d increases, in the ipsilateral anterior middle frontal gyrus ($Z = 4.53$, $k = 356$, $P = 0.005$) and in the contralateral angular gyrus ($Z = 4.12$, $k = 298$, $P = 0.012$), both at the GM–WM interface. In the *post hoc* analysis, a small area of increased binding was seen medial to the contralateral ventricle centrally.

Occipital lobe epilepsy

Individual patients (see Table 1)

Two patients (O2 and O4) had no significant abnormalities at conventional thresholds. One patient (O3), without clear lateralization of her focus, had an area of increased FMZ-V_d in one inferior parietal lobe and another one in the frontal lobe on the other side. Two patients (O1 and O5) showed decreases only, one (O1) in the ipsilateral and contralateral medial occipital lobe and the other (O5) in the contralateral precentral gyrus. No patient had periventricular increases at conventional thresholds.

The *post hoc* analysis revealed periventricular increases in all five patients, including the two in whom no abnormality had been found previously (see Table 1). The periventricular increases in the *post hoc* analysis included, alone or in combination, the anterior horn in one, central periventricular areas in three out of five and the posterior horn in four out of five.

Group analysis

As only two patients (O1 and O5) had clearly lateralized OLE, all patients' unflipped normalized and smoothed scans were included in the group analysis. There was one cluster of significantly decreased FMZ-V_d in the left middle cingulate gyrus ($Z = 4.05$, $k = 228$, $P = 0.026$). The *post hoc* analysis showed bilateral central and right posterior periventricular increases.

Neocortical epilepsy, not clearly unilobar

Individual patients (see Table 1)

Five patients (X6, X7, X11, X15 and X17) had no significant abnormalities at conventional thresholds.

Six had areas of increased FMZ-V_d only; two had single areas of increased FMZ binding (X16 and X18) and four had more than one area of increased FMZ-V_d (X4, X9, X13 and X19). The latter included two of the three patients in this group with periventricular increases at conventional thresholds (X2, X4 and X19). Three patients had areas of decreased FMZ binding only; one had a single area of decreased FMZ-V_d (X14), and two had more than one area (X1 and X8). Five patients showed both increases and decreases (X2, X3, X5, X10 and X12). In total, in nine of the 14 patients with abnormalities, these included the area of presumed seizure onset. Figure 3 shows an example of a patient with a decrease of GM binding (X12).

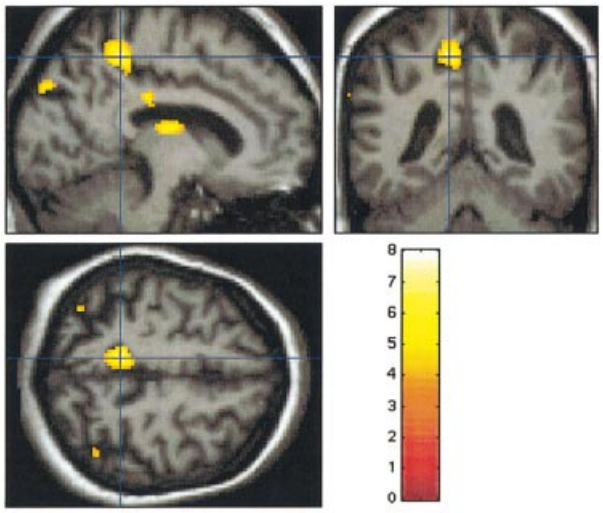

Fig. 3 Example of a patient (X12) with decreased FMZ-V_d in the left inferior postcentral gyrus. Colour scale: *t* score. Statistical results are overlaid onto the patient's co-registered MRI. Only the cluster marked with the crosshair is significant [maximum $t = 7.39$, corresponding to $Z = 4.56$; cluster size 325 voxels, P corrected = 0.002; peak coordinates in MNI/ICBM space ($x/y/z$) = –10/–44/54].

The *post hoc* analysis revealed periventricular increases in 16 out of 19 patients, including four of the five in whom no abnormality had been found previously (see Table 1). One patient's (X11) FMZ PET did not show any abnormality at all, and the two others (X9 and X13) had areas of increased FMZ binding elsewhere which included areas of WM. The periventricular increases in the *post hoc* analysis included, alone or in combination, the anterior horn in seven out of 16, central periventricular areas in 14 out of 16 and the posterior horn in five out of 16.

Correlation with clinical data

There was no correlation between duration of epilepsy, age at onset of seizures, frequency of seizures, interval between last seizure and PET scan and FMZ binding anywhere in the brain.

Exclusion of artefacts

Exclusion of chance effects through composition of the control group

Comparing patient F4, with significant periventricular increases of FMZ binding at conventional thresholds, against a different control group as described in the Methods showed essentially the same significant clusters around the ventricles, with very similar *Z* scores, extents and *P* values. Our finding of periventricular increases was not, therefore, dependent on the composition of the control group.

Exclusion of flipping artefacts in the group analyses

In both groups (unilateral FLE and PLE) in which the group analysis was repeated after flipping the other half of the raw images before normalization to our symmetrical template, we obtained the same results. Thus, potential flipping artefacts did not influence our results.

Exclusion of normalization artefacts through verification with ROI analysis

ROI analysis in patient X4, with significant periventricular increases of FMZ binding at conventional thresholds in the SPM analysis, showed a significant increase in bilateral periventricular ROIs. This was +114% for the left periventricular area and +102% for the right periventricular area (control mean ± SD ROI value 0.57 ± 0.10, patient ROI value 1.15 ± 0.75 on the right and 1.22 ± 0.5 on the left). Our findings are therefore not due to artefacts arising from the manipulation of data sets for analysis with SPM99 (see also Fig. 4).

Surgical and histological results; outcome

So far, one patient has had surgery. Patient F11 with an electroclinical diagnosis of right FLE had multiple areas of increased FMZ-V_d including the right frontal lobe. Diffusion tensor imaging, analysed with SPM99 against a control group of 30 subjects, showed an increase in mean diffusivity in the right orbitofrontal WM (Rugg-Gunn *et al*., 2001). Depth electrodes in orbitofrontal and inferior lateral frontal cortex demonstrated very localized onset of ictal activity. This area subsequently was surgically removed, and the patient has had a >90% reduction of seizures over the 18 months of postoperative follow-up. Pathology showed marked WM gliosis. One section was selected randomly, sectioned at 20 μm and stained with the neuronal marker, neuronal nuclear antigen (NeuN). All NeuN-positive cells, i.e. all neurons, were counted in radial columns in WM using a 3D cell counting technique as described recently (Thom *et al*., 2001). WM neuronal density was estimated at 1598/mm^3.

Discussion

This is the first study to examine explicitly both GM and WM changes in FMZ-V_d in patients with neocortical focal epilepsies and normal high resolution MRI. The main novel finding is the high proportion of patients with increased WM FMZ binding, notably around the ventricles, and we suggest that this finding represents a disorder of neuronal migration which is aetiologically and clinically relevant.

In total, we found abnormalities in 33 out of 44 patients with partial epilepsy and normal optimal MRI, confirming that [^{11}C]FMZ PET detects abnormalities over and above structural MRI-visible abnormalities.

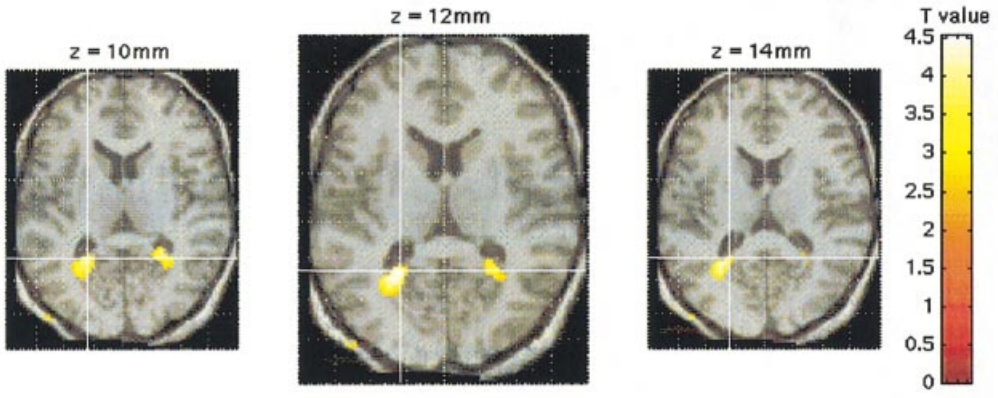

Fig. 4 Example of an SPM of a patient with unilateral subependymal periventricular nodular heterotopia on MRI (patient 7 from Hammers *et al*., 2002*b*), using exactly the same technique as in the remainder of the patients in this study. The patient showed the expected ipsilateral (right; left on image) periventricular increase of FMZ-V_d, corresponding to the periventricular nodular heterotopia confirmed on MRI. Furthermore, SPM reveals a contralateral (left; right on image) area of increased periventricular FMZ-V_d which had no correlate on MRI, but corresponds equally well to the appearance of periventricular increases in the current study.

Methodological considerations

SPM is a voxel-based analysis technique that examines the entire data set and has been validated for the interpretation of ligand PET scans in epilepsy (Koepp *et al*., 1996, 2000; Richardson *et al*., 1997, 1998*b*). SPM cannot differentiate between abnormalities due to structural alterations or purely functional abnormalities. Therefore, in this study, we only included patients whose high quality MRI including a variety of sequences was normal on inspection by two experienced neuroradiologists. In this situation, SPM has advantages over region-based analyses: the entire brain volume can be studied, and no assumptions about number, localization and extent of abnormalities need to be made. A disadvantage is the decrease of the spatial resolution of the resulting statistical map to ~13 mm FWHM, owing to the necessary interpolations following spatial manipulation and the smoothing procedure to accommodate inter-individual anatomical differences. The final spatial resolution of region-based analyses, however, depends on the number and size of regions chosen (typically 10–50 for a given brain imaging data set), whereas at our level of smoothing, SPM examines the data with ~500 independent comparisons. Furthermore, no *a priori* hypotheses about the exact localization of abnormalities need to be made. As in our previous studies, the validity of our approach was tested empirically through investigation of each control against the remaining controls. This gives a good empirical verification of the false-positive rate expected as all healthy controls should *a priori* have normal FMZ-V_d, and the expected number of false positives was found.

SPM needs rigorous correction for the multiple comparisons made. If such a correction is applied to the entire volume, abnormalities of small magnitude or extent will remain undetected. We found periventricular increases in a substantial number of patients at conventional thresholds, but in none of the controls. To explore periventricular changes further, we defined an additional mask for the periventricular areas for a *post hoc* analysis. This mask was defined as the average location of the ventricles in the stereotactic space used three-dimensionally dilated by 5 mm, and therefore allowed an objective search procedure for such changes. Within this defined search volume, we did not correct for the spatial extent of the clusters of abnormal FMZ binding, but only for height, as in our previous studies (Koepp *et al*., 2000; Hammers *et al*., 2001*a*). With this approach, five out of 16 controls showed periventricular increases compared with 38 out of 44 patients (χ^2 test: $P < 0.0001$).

We took great care to exclude potential artefacts as the source of our findings, and are confident that methodological issues are not responsible for them, including WM volume decreases (and corresponding CSF volume increases). Even if they were present to a degree that could have not been noted by the neuroradiological reviewers of the MRI data, their presence would have led to an underestimation, not overestimation, of periventricular FMZ binding in both SPM and the ROI analysis.

FMZ PET revealed periventricular binding increases which did not correspond to MRI changes, even after the MRIs were re-examined in the light of the FMZ PET findings. Even though the signal to noise ratio is generally lower for PET than for MRI, the greater ability of FMZ PET to detect abnormalities in this situation with its femtomolar sensitivity can be explained through the better contrast to noise ratio. FMZ binds highly specifically to $GABA_A$ receptors with α-subunits 1, 2, 3 or 5, present on the soma of most neurons but not on myelinated axons. Even slightly or diffusely increased average numbers of neurons per unit of WM in the periventricular area will thus lead to a detectable increase of FMZ-V_d, whereas clusters of neurons <1 mm^3 would not be detectable on current MRI.

Comparison with previous findings

Earlier studies have provided extensive evidence that decreased FMZ binding can localize the epileptogenic focus in both mesial TLE and neocortical epilepsy (Savic *et al*., 1988, 1993, 1995; Henry *et al*., 1993; Koepp *et al*., 1996, 1997*b*; Szelies *et al*., 1996; Ryvlin *et al*., 1998; Muzik *et al*., 2000; Juhász *et al*., 2001). Decreased FMZ binding may be related to structural pathology as found in areas of past acute and non-progressive cerebral injury (Richardson *et al*., 1998*b*). Decreased FMZ binding can, however, indicate functional abnormalities over and above evident structural abnormalities (Henry *et al*., 1993; Koepp *et al*., 1997*a*,*b*, 2000; Hammers *et al*., 2001*a*) which represents the rationale for using FMZ PET in patients with normal structural imaging, as in the present study.

Increased FMZ binding is difficult to detect on region-based analyses using measures of asymmetry, and may be more difficult to see on visual inspection (Hammers *et al*., 2001*a*). Using quantified parametric images of FMZ binding and comparisons with control groups, however, we previously have shown areas of increased binding in patients with MCDs (Richardson *et al*., 1996, 1997; Hammers *et al*., 2001*b*). Similar increases were found in patients with neocortical epilepsy and normal MRI, but in none of six patients with epilepsy clearly due to acquired non-progressive lesions (Richardson *et al*., 1998*b*), leading to the hypothesis that malformations not evident on MRI may be the basis of increased FMZ binding.

We recently have found a strong correlation ($r > 0.8$, $P < 0.001$) between preoperative WM FMZ-V_d in both temporal lobes and the WM neuron number determined in the resected ipsilateral specimen in patients with hippocampal sclerosis (Hammers *et al*., 2001*a*). Increased neuron number in the TLWM is a hallmark of microdysgenesis. Using the same technique as described here, we subsequently found TLWM increases, presumably indicating microdysgenesis, in a group of 18 patients with TLE and normal qualitative and quantitative MRI, as well as in 11 out of 18 individual patients (Hammers *et al*., 2002*b*). We found a high frequency (25 out of 44) of increases of FMZ binding in the current study in patients with neocortical epilepsy and normal MRI, often including WM or, as in the case of the periventricular increases, located exclusively within the WM.

To keep the number of voxels studied to a minimum, in SPM, WM is normally excluded from the analysis through thresholding. If this blanket threshold is simply lowered to include WM signal, results are inconsistent due to the inter-individual variability in global binding. Further, the number of voxels included in the analysis is unnecessarily increased around the outer border of the brain image, thereby accentuating the multiple comparisons problem. We therefore created an anatomical mask in stereotactic space, encompassing the GM in the cortex and in the basal ganglia as well as central WM. This enabled us to study explicitly, for the first time, WM changes while restricting the number of voxels inspected.

The sensitivity of our technique to detect cortical (GM) abnormalities could be reduced due to the increased number of comparisons involved in also studying WM. One previous study that included patients with neocortical epilepsies used similar inclusion criteria and a similarly stringent definition of normal MRI studies (Ryvlin *et al*., 1998); however, decreased [^{11}C]FMZ binding was present in some 12 out of 30 (40%) of patients, comparable with 17 out of 44 (39%) in our series. Similarly, the number of focal decreases considered useful was only two out of 11 (18%) in their unilateral FLE patients. Some earlier studies are not comparable due to selection bias as they specifically excluded patients who did not proceed to undergo epilepsy surgery (Muzik *et al*., 2000; Juhász *et al*., 2001), or indeed excluded patients with no abnormalities on FMZ PET (Juhász *et al*., 2001). Another study with a higher rate of abnormalities found on FMZ PET used MRI on different low field strength machines with very thick slices (Savic *et al*., 1995). These sequences are no longer recommended in the pre-surgical evaluation of patients with refractory epilepsy (Commission on Neuroimaging of the International League Against Epilepsy, 1998), and the lower yield in our study is almost certainly due to the advances made in MRI imaging over the past decade, rather than our method of analysis of FMZ binding.

Neurobiological considerations

Our finding of areas of decreased FMZ binding, alone in eight out of 44 patients and in combination with areas of increased FMZ binding in a further nine out of 44, replicates earlier findings in both mesial TLE and neocortical epilepsy (Savic *et al*., 1988, 1993, 1995; Henry *et al*., 1993; Koepp *et al*., 1996, 1997*b*; Szelies *et al*., 1996; Ryvlin *et al*., 1998; Muzik *et al*., 2000; Juhász *et al*., 2001). Such decreases may indicate a loss of $GABA_A$ receptors, loss of $GABA_A$ receptor-bearing cells, or a change in subunit composition (Brooks-Kayal *et al*., 1998; Sperk *et al*., 1998; Loup *et al*., 2000) with ensuing reduction of affinity (Nagy *et al*., 1999).

Cortical increases of FMZ binding may be due to an increase in $GABA_A$ receptor density, an increased neuronal density or ectopic neurons bearing $GABA_A$ receptors, as for example in microdysgenesis. The dysgenesis hypothesis is supported by the fact that cortical increases of FMZ-V_d have only been observed in patients with MCDs, including areas of cortex appearing normal on MRI (Richardson *et al*., 1996, 1997), in 'MRI-negative' patients (Richardson *et al*., 1998*b*; Koepp *et al*., 2000; Muzik *et al*., 2000) and in patients with hippocampal sclerosis with associated microdysgenesis (Hammers *et al*., 2001*a*), but not in acquired epilepsies (Richardson *et al*., 1998*b*).

Subcortical WM increases of FMZ binding are best explained by increased numbers of WM neurons (Hammers *et al*., 2001*a*). FMZ PET is well suited to determine abnormal nerve cell content in the WM *in vivo*: most neurons express $GABA_A$ receptors. FMZ can,

therefore, be regarded to a certain extent as a neuronal marker, and the contrast to noise ratio for ectopic neurons in the WM is very high.

Ectopic WM neurons might contribute to epileptogenesis by providing additional or abnormal connections between nerve cells, as shown experimentally for ectopic CA1 (cornu ammonis subfield 1) neurons in the rat model of methylazoxymethanol (MAM)-induced cortical malformations (Chevassus-au-Louis *et al*., 1998). Human tissue is scarce, as patients with malformations are less suitable for epilepsy surgery (Sisodiya, 2000), but there is direct evidence for connectivity of ectopic GM from both autopsy cases (Hannan *et al*., 1999) and functional imaging studies (Richardson *et al*., 1998*a*; Pinard *et al*., 2000; Spreer *et al*., 2001), and evidence for epileptogenicity of periventricular neuronal clusters (Francione *et al*., 1994; Mattia *et al*., 1995; Palmini *et al*., 1995; Sisodiya *et al*., 1999). The finding of ectopic WM neurons in neocortical focal epilepsy with normal MRI is therefore a tenable explanation for the pathogenesis of epileptic circuits. Further, the periventricular increases tended to be more anterior in the cases of FLE and more posterior in the PLE and OLE groups, in keeping with the clinical semiology of the patients' seizures and our prior classification.

Microdysgenesis has been defined in different ways, and this accounts partly for the controversies surrounding its relevance in epilepsy (Meencke and Janz, 1984, 1985; Lyon and Gastaut, 1985). Increased WM neuron numbers, however, are regularly included in the definition (Raymond *et al*., 1995). It is evident that there is a rather wide range of normal variation (Hardiman *et al*., 1988; Rojiani *et al*., 1996; Emery *et al*., 1997; Kasper *et al*., 1999; Thom *et al*., 2001), there is major regional variation (Rojiani *et al*., 1996), and more neurons are found in periventricular areas compared with subcortical WM (Thom *et al*., 2001). In the current study, increased FMZ binding in periventricular WM was present in seven out of 44 patients and in none of the 16 controls at conventional thresholds. In the *post hoc* analysis of the periventricular areas, 38 out of 44 patients versus five out of 16 controls showed such increases (χ^2 test: $P < 0.0001$), further underlining the relevance of our findings for the pathophysiology of epilepsy.

The quantitative ROI analysis showed an ~100% increase in FMZ-V_d around the posterior horns in a case of periventricular increases, compared with the corresponding area in controls. As we determined the effect size in a very clear-cut case, the order of magnitude of the changes is compatible with previous pathological studies of average increases in WM neurons in temporal lobe specimens obtained at surgery for refractory TLE, which showed increases of 30–75% (Emery *et al*., 1997; Thom *et al*., 2001).

Only one patient has been operated upon so far. One cluster of significantly increased FMZ binding in the right orbitofrontal WM was included in the resection. Quantitative immunohistochemistry (Thom *et al*., 2001) with NeuN estimated the neuronal density in a randomly selected section of the WM at 1598/mm^3, near the mean neuronal WM density in temporal lobe in controls as determined with the same method (Thom *et al*., 2001). We do not yet have other frontal lobe specimens. As the number of heterotopic neurons in normal subjects, however, has been found to be 6.2 times higher in temporal lobe WM compared with frontal lobe WM, with no overlap of the normal ranges (Rojiani *et al*., 1996), the finding of a neuronal density in the middle of the normal range for temporal lobe in our frontal lobe specimen infers a large increase in neuronal density compared with controls. This provides further evidence for the possibility of microdysgenesis as the neurobiological basis for our PET findings.

Clinical considerations

Patients with normal MRI and medically refractory neocortical focal epilepsy represent a very important and difficult subgroup of patients who undergo investigations for epilepsy surgery. Accordingly, there have been various FMZ PET studies including MRI-negative patients (Savic *et al*., 1988, 1993, 1995; Henry *et al*., 1993; Szelies *et al*., 1996; Debets *et al*., 1997; Richardson *et al*., 1998*b*; Ryvlin *et al*., 1998; Koepp *et al*., 2000; Lamusuo *et al*., 2000; Muzik *et al*., 2000; Juhász *et al*., 2001) (see also the section on comparison with previous findings, above). Most of the earlier studies used ROI approaches with limited numbers of volumes of interest or relied on measures of asymmetry for FMZ binding, and could not therefore detect bilateral abnormalities. No previous studies have explicitly included WM.

If our finding of frequent and mostly bilateral periventricular abnormalities can be confirmed, this would represent an important addition to the non-invasive pre-surgical evaluation. Such a finding would make it very unlikely that a patient would become seizure free after a focal resection (Li *et al*., 1997; Sisodiya, 2000) and could be a reason for not pursuing the evaluation further, if a less than seizure-free outcome would be regarded as a failure.

The patient in this series who has so far been operated upon (F11) might be a case in point. On electroclinical grounds, she was suspected to have right FLE. Diffusion tensor imaging showed right orbitofrontal abnormalities (Rugg-Gunn *et al*., 2001). Intracranial recordings showed onset of typical attacks from just one electrode over the right orbitofrontal cortex, and she underwent a partial right frontal lobe resection. Although she benefitted from surgery with a >90% reduction of seizures over the 18 month of postoperative follow-up so far, her seizures have not been controlled fully through surgery. The result of the present study, which became available later, suggested widespread abnormalities of FMZ binding, involving mainly both frontal lobes and consisting of increases involving both GM and WM. Moreover, in the *post hoc* analysis, she showed bilateral periventricular increases of FMZ binding, further indicating more widespread abnormalities.

Large or remote abnormalities of FMZ PET are a very common finding in MRI-negative patients even when only patients undergoing surgery are included (Muzik *et al*., 2000; Juhász *et al*., 2001). When MRI-negative patients are operated upon, outcome is known to be worse than when a lesion is present on MRI in TLE (Jack *et al*., 1992; Berkovic *et al*., 1995), and poorer outcome has been found to be associated with the size of abnormalities on FMZ PET and the proportion of non-resected abnormalities on FMZ PET in extratemporal epilepsies (Muzik *et al*., 2000; Juhász *et al*., 2001).

In the current series, nine out of 44 cases had single focal abnormalities of FMZ binding at conventional thresholds, but in only one of these cases were no periventricular increases of FMZ binding seen in the *post hoc* analysis. Single abnormalities are potential targets for invasive EEG monitoring to confirm whether this is the site of seizure onset. Further prospective studies are needed to determine the concordance between FMZ PET abnormalities in GM with invasive EEG recordings and follow-up following surgical resection, in patients with refractory focal neocortical epilepsy and normal MRI. Such studies are also needed to determine whether periventricular abnormalities of FMZ binding are a predictor of outcome following epilepsy surgery or not.

Acknowledgements

We wish to thank our colleagues at the MRC Cyclotron Building (particularly Andrew Blyth, Joanne Holmes, Leonhard Schnorr and Drs Richard Banati, Peter Bloomfield, Matthew Brett, Annachiara Cagnin, Roger Gunn, Ralph Myers and Federico Turkheimer) for help in the acquisition and analysis of PET data; Professors Ley Sander, Simon Shorvon and David Fish, Drs Chrysostomos Panayiotopoulos, Sanjay Sisodiya and Shelagh Smith, and Catherine Scott for referring patients, Professor David Fish, Dr Shelagh Smith and the EEG technicians at the National Hospital and the National Society for Epilepsy for acquiring and reporting the EEG and video-EEG data, Mr William Harkness for performing the surgical resection, Dr Maria Thom at the Institute of Neurology for performing the three-dimensional WM cell counts, our colleagues at the National Society for Epilepsy for performing, reporting and transferring the MRI scans, and William Horner for artistic assistance. Action Research (SP 3123), the National Society for Epilepsy, the Medical Research Council and the Deutsche Forschungsgemeinschaft (Ha 3013/1-1) supported this research.

References

Ashburner J, Friston KJ. Multimodal image coregistration and partitioning—a unified framework. Neuroimage 1997; 6: 209–17.

Ashburner J, Friston KJ. Nonlinear spatial normalization using basis functions. Hum Brain Mapp 1999; 7: 254–66.

Bailey DL. 3D acquisition and reconstruction in positron emission tomography. Ann Nucl Med 1992; 6: 121–30.

Berkovic SF, McIntosh AM, Kalnins RM, Jackson GD, Fabinyi GC, Brazenor GA, et al. Preoperative MRI predicts outcome of temporal lobectomy: an actuarial analysis. Neurology 1995; 45: 1358–63.

Brooks-Kayal AR, Shumate MD, Jin H, Rikhter TY, Coulter DA. Selective changes in single cell $GABA_A$ receptor subunit expression and function in temporal lobe epilepsy. Nat Med 1998; 4: 1166–72.

Chevassus-au-Louis N, Congar P, Represa A, Ben-Ari Y, Gaiarsa J-L. Neuronal migration disorders: heterotopic neocortical neurons in CA1 provide a bridge between the hippocampus and the neocortex. Proc Natl Acad Sci USA 1998; 95: 10263–8.

Chugani HT, Shields WD, Shewmon DA, Olson DM, Phelps ME, Peacock WJ. Infantile spasms: I. PET identifies focal cortical dysgenesis in cryptogenic cases for surgical treatment. Ann Neurol 1990; 27: 406–13.

Commission on Neuroimaging of the International League Against Epilepsy. Guidelines for neuroimaging evaluation of patients with uncontrolled epilepsy considered for surgery. Epilepsia 1998; 39: 1375–6.

Cunningham VJ, Jones T. Spectral analysis of dynamic PET studies. J Cereb Blood Flow Metab 1993; 13: 15–23.

Debets RMC, Sadzot B, van Isselt JW, Brekelmans GJF, Meiners LC, van Huffelen AO, et al. Is ^{11}C-flumazenil PET superior to ^{18}FDG PET and ^{123}I-iomazenil SPECT in presurgical evaluation of temporal lobe epilepsy? J Neurol Neurosurg Psychiatry 1997; 62: 141–50.

Desbiens R, Berkovic SF, Dubeau F, Andermann F, Laxer KD, Harvey S, et al. Life-threatening focal status epilepticus due to occult cortical dysplasia. Arch Neurol 1993; 50: 695–700.

Dubeau F, Tampieri D, Lee N, Andermann E, Carpenter S, Leblanc R, et al. Periventricular and subcortical nodular heterotopia. A study of 33 patients. Brain 1995; 118: 1273–87.

Duncan JS. Imaging and epilepsy. Brain 1997; 120: 339–77.

Emery JA, Roper SN, Rojiani AM. White matter neuronal heterotopia in temporal lobe epilepsy: a morphometric and immunohistochemical study. J Neuropathol Exp Neurol 1997; 56: 1276–82.

Francione S, Kahane P, Tassi L, Hoffmann D, Durisotti C, Pasquier B, et al. Stereo-EEG of interictal and ictal electrical activity of a histologically proved heterotopic gray matter associated with partial epilepsy. Electroencephalogr Clin Neurophysiol 1994; 90: 284–90.

Friston KJ, Frith CD, Liddle PF, Dolan RJ, Lammertsma AA, Frackowiak RS. The relationship between global and local changes in PET scans. J Cereb Blood Flow Metab 1990; 10: 458–66.

Friston KJ, Frith CD, Liddle PF, Frackowiak RS. Comparing functional (PET) images: the assessment of significant change. J Cereb Blood Flow Metab 1991; 11: 690–9.

Friston KJ, Ashburner J, Frith CD, Poline JB, Heather JD, Frackowiak RS. Spatial registration and normalization of images. Hum Brain Mapp 1995*a*; 3: 165–189.

Friston KJ, Holmes AP, Worsley KJ, Poline JB, Frith CD, Frackowiak RSJ. Statistical parametric maps in functional imaging: a general linear approach. Hum Brain Mapp 1995*b*; 2: 189–210.

Grootoonk S. Dual energy window correction for scattered photons in 3D positron emission tomography [PhD thesis]. Guildford (UK): University of Surrey; 1995.

Hammers A, Koepp MJ, Labbé C, Brooks DJ, Thom M, Cunningham VJ, et al. Neocortical abnormalities of [^{11}C]-flumazenil PET in mesial temporal lobe epilepsy. Neurology 2001*a*; 56: 897–906.

Hammers A, Koepp MJ, Richardson MP, Labbé C, Brooks DJ, Cunningham VJ, et al. Central benzodiazepine receptors in malformations of cortical development. A quantitative study. Brain 2001*b*; 124: 1555–65.

Hammers A, Koepp MJ, Free SL, Brett M, Richardson MP, Labbé C, et al. Implementation and application of a brain template for multiple volumes of interest. Hum Brain Mapp 2002*a*; 15: 165–74.

Hammers A, Koepp MJ, Hurlemann R, Thom M, Richardson MP, Brooks DJ, et al. Abnormalities of grey and white matter [^{11}C]flumazenil binding in temporal lobe epilepsy with normal MRI. Brain 2002*b*; 125: 2257–71.

Hand KS, Baird VH, Van Paesschen W, Koepp MJ, Revesz T, Thom M, et al. Central benzodiazepine receptor autoradiography in hippocampal sclerosis. Br J Pharmacolol 1997; 122: 358–64.

Hannan AJ, Servotte S, Katsnelson A, Sisodiya S, Blakemore C, Squier M, et al. Characterization of nodular neuronal heterotopia in children. Brain 1999; 122: 219–38.

Hardiman O, Burke T, Phillips J, Murphy S, O'Moore B, Staunton H, et al. Microdysgenesis in resected temporal neocortex: incidence and clinical significance in focal epilepsy. Neurology 1988; 38: 1041–7.

Henry TR, Frey KA, Sackellares JC, Gilman S, Koeppe RA, Brunberg JA, et al. In vivo cerebral metabolism and central benzodiazepine-receptor binding in temporal lobe epilepsy. Neurology 1993; 43: 1998–2006.

Jack CR Jr, Sharbrough FW, Cascino GD, Hirschorn KA, O'Brien PC, Marsh WR. Magnetic resonance image-based hippocampal volumetry: correlation with outcome after temporal lobectomy. Ann Neurol 1992; 31: 138–146.

Juhász C, Chugani DC, Muzik O, Shah A, Shah J, Watson C, et al. Relationship of flumazenil and glucose PET abnormalities to neocortical epilepsy surgery outcome. Neurology 2001; 56: 1650–1658.

Kasper BS, Stefan H, Buchfelder M, Paulus W. Temporal lobe microdysgenesis in epilepsy versus control brains. J Neuropathol Exp Neurol 1999; 58: 22–8.

Koepp MJ, Richardson MP, Brooks DJ, Poline JB, Van Paesschen W, Friston KJ, et al. Cerebral benzodiazepine receptors in hippocampal sclerosis. An objective in vivo analysis. Brain 1996; 119: 1677–1687.

Koepp MJ, Labbé C, Richardson MP, Brooks DJ, Van Paesschen W, Cunningham VJ, et al. Regional hippocampal [11C]flumazenil PET in temporal lobe epilepsy with unilateral and bilateral hippocampal sclerosis. Brain 1997*a*; 120: 1865–1876.

Koepp MJ, Richardson MP, Labbé C, Brooks DJ, Cunningham VJ, Ashburner J, et al. 11C-flumazenil PET, volumetric MRI, and quantitative pathology in mesial temporal lobe epilepsy. Neurology 1997*b*; 49: 764–773.

Koepp MJ, Hammers A, Labbé C, Wörmann FG, Brooks DJ, Duncan JS. ^{11}C-flumazenil PET in patients with refractory temporal lobe epilepsy and normal MRI. Neurology 2000; 54: 332–9.

Koeppe RA, Holthoff VA, Frey KA, Kilbourn MR, Kuhl DE. Compartmental analysis of [^{11}C] flumazenil kinetics for the estimation of ligand transport rate and receptor distribution using positron emission tomography. J Cereb Blood Flow Metab 1991; 11: 735–744.

Kuzniecky RI, Jackson GD. Developmental disorders. In: Engel JJ Jr, Pedley TA, editors. Epilepsy: a comprehensive textbook. Philadelphia: Lippincott-Raven; 1997. p. 2517–32.

Kuzniecky R, Garcia JH, Faught E, Morawetz RB. Cortical dysplasia in temporal lobe epilepsy: magnetic resonance imaging correlations. Ann Neurol 1991; 29: 293–8.

Kwan P, Brodie MJ. Early identification of refractory epilepsy. N Engl J Med 2000; 342: 314–9.

Lammertsma AA, Lassen NA, Prevett MC, Bartenstein PA, Turton DR, Luthra SK, et al. Quantification of benzodiazepine receptors in vivo using [11C]flumazenil: application of the steady state principle. In: Uemura K, Lasson NA, Jones T, Kanno I, editors. Quantification of brain function. Tracer kinetics and image analysis in brain PET. Amsterdam: Elsevier Science; 1993. p. 303–11.

Lamusuo S, Pitkänen A, Jutila L, Ylinin A, Partanen K, Kälviäinen R, et al. [^{11}C]Flumazenil binding in the medial temporal lobe in patients with temporal lobe epilepsy. Correlation with hippocampal MR volumetry, T2 relaxometry, and neuropathology. Neurology 2000; 54: 2252–60.

Li LM, Dubeau F, Andermann F, Fish DR, Watson C, Cascino GD, et al. Periventricular nodular heterotopia and intractable temporal lobe epilepsy: poor outcome after temporal lobe resection. Ann Neurol 1997; 41: 662–8.

Loup F, Wieser HG, Yonekawa Y, Aguzzi A, Fritschy JM. Selective alterations in GABAA receptor subtypes in human temporal lobe epilepsy. J Neurosci 2000; 20: 5401–5419.

Lyon G, Gastaut M. Considerations on the significance attributed to unusual cerebral histological findings recently described in eight patients with primary generalized epilepsy. Epilepsia 1985; 26: 365–367.

Mattia D, Olivier A, Avoli M. Seizure-like discharges recorded in human dysplastic neocortex maintained *in vitro*. Neurology 1995; 45: 1391–5.

Maziere M, Hantraye P, Prenant C, Sastre J, Comar D. Synthesis of an ethyl 8-fluoro-5,6-dihydro-5-[11C]methyl-6-oxo-4H-imidazo[1,5-a][1,4]benzodiazepine-3-carboxylate (RO 15.1788-11C): a specific radioligand for the in vivo study of central benzodiazepine receptors by positron emission tomography. Int J Appl Radiat Isot 1984; 35: 973–6.

Meencke HJ, Janz D. Neuropathological findings in primary

generalized epilepsy: a study of eight cases. Epilepsia 1984; 25: 8–21.

Meencke HJ, Janz D. The significance of microdysgenesia in primary generalized epilepsy: an answer to the considerations of Lyon and Gastaut. Epilepsia 1985; 26: 368–71.

Muzik O, da Silva EA, Juhász C, Chugani DC, Shah J, Nagy F, et al. Intracranial EEG versus flumazenil and glucose PET in children with extratemporal lobe epilepsy. Neurology 2000; 54: 171–9.

Nagy F, Chugani DC, Juhász C, da Silva EA, Muzik O, Kupsky W, et al. Altered *in vitro* and *in vivo* flumazenil binding in human epileptogenic neocortex. J Cereb Blood Flow Metab 1999; 19: 939–47.

Olsen RW, McCabe RT, Wamsley JK. $GABA_A$ receptor subtypes: autoradiographic comparison of GABA, benzodiazepine, and convulsant binding sites in the rat central nervous system. J Chem Neuroanat 1990; 3: 59–76.

Palmini A, Gambardella A, Andermann F, Dubeau F, da Costa JC, Olivier A, et al. Intrinsic epileptogenicity of human dysplastic cortex as suggested by corticography and surgical results. Ann Neurol 1995; 37: 476–87.

Pinard J-M, Feydy A, Carlier R, Perez N, Pierot L, Burnod Y. Functional MRI in double cortex: functionality of heterotopia. Neurology 2000; 54: 1531–3.

Raymond AA, Fish DR, Stevens JM, Sisodiya SM, Alsanjari N, Shorvon SD. Subependymal heterotopia: a distinct neuronal migration disorder associated with epilepsy. J Neurol Neurosurg Psychiatry 1994; 57: 1195–202.

Raymond AA, Fish DR, Sisodiya SM, Alsanjari N, Stevens JM, Shorvon SD. Abnormalities of gyration, heterotopias, tuberous sclerosis, focal cortical dysplasia, microdysgenesis, dysembryoplastic neuroepithelial tumour and dysgenesis of the archicortex in epilepsy. Clinical, EEG and neuroimaging features in 100 adult patients. Brain 1995; 118: 629–60.

Richardson MP, Koepp MJ, Brooks DJ, Fish DF, Duncan JS. Benzodiazepine receptors in focal epilepsy with cortical dysgenesis: an ^{11}C-flumazenil PET study. Ann Neurol 1996; 40: 188–198.

Richardson MP, Friston KJ, Sisodiya SM, Koepp MJ, Ashburner J, Free SL, et al. Cortical grey matter and benzodiazepine receptors in malformations of cortical development. A voxel-based comparison of structural and functional imaging data. Brain 1997; 120: 1961–73.

Richardson MP, Koepp MJ, Brooks DJ, Coull JT, Grasby P, Fish DR, et al. Cerebral activation in malformations of cortical development. Brain 1998*a*; 121: 1295–304.

Richardson MP, Koepp MJ, Brooks DJ, Duncan JS. ^{11}C-flumazenil PET in neocortical epilepsy. Neurology 1998*b*; 51: 485–492.

Rojiani AM, Emery JA, Anderson KJ, Massey JK. Distribution of heterotopic neurons in normal hemispheric white matter: a morphometric analysis. J Neuropathol Exp Neurol 1996; 55: 178–83.

Rugg-Gunn FJ, Eriksson SH, Symms MR, Barker GJ, Duncan JS. Diffusion tensor imaging of cryptogenic and acquired partial epilepsies. Brain 2001; 124: 627–36.

Ryvlin P, Bouvard S, Le Bars D, De Lamérie G, Grégoire MC, Kahane P, et al. Clinical utility of flumazenil-PET versus [^{18}F]fluorodeoxyglucose-PET and MRI in refractory partial epilepsy. A prospective study in 100 patients. Brain 1998; 121: 2067–81.

Savic I, Persson A, Roland P, Pauli S, Sedvall G, Widen L. In-vivo demonstration of reduced benzodiazepine receptor binding in human epileptic foci. Lancet 1988; 2: 863–6.

Savic I, Ingvar M, Stone-Elander S. Comparison of 11C-flumazenil and 18F-FDG as PET markers of epileptic foci. J Neurol Neurosurg Psychiatry 1993; 56: 615–21.

Savic I, Thorell JO, Roland P. [11C]flumazenil positron emission tomography visualises frontal epileptogenic regions. Epilepsia 1995; 36: 1225–32.

Sisodiya SM. Surgery for malformations of cortical development causing epilepsy. Brain 2000; 123: 1075–91.

Sisodiya SM, Free SL, Thom M, Everitt AE, Fish DR, Shorvon SD. Evidence for nodular epileptogenicity and gender differences in periventricular nodular heterotopia. Neurology 1999; 52: 336–41.

Sperk G, Schwarzer C, Tsunashima K, Kandlhofer S. Expression of $GABA_A$ receptor subunits in the hippocampus of the rat after kainic acid-induced seizures. Epilepsy Res 1998; 32: 129–39.

Spreer J, Martin P, Greenlee MW, Wohlfarth R, Hammen A, Arnold SM, et al. Functional MRI in patients with band heterotopia. Neuroimage 2001; 14: 357–65.

Szelies B, Weber-Luxenburger G, Pawlik G, Kessler J, Holthoff V, Mielke R, et al. MRI-guided flumazenil- and FDG-PET in temporal lobe epilepsy. Neuroimage 1996; 3: 109–18.

Talairach J, Tournoux P. Co-planar stereotaxic atlas of the human brain. Stuttgart: Thieme; 1988.

Thom M, Sisodiya SM, Harkness WF, Scaravilli F. Microdysgenesis in temporal lobe epilepsy: a quantitative and immunohistochemical study of white matter neurones. Brain 2001; 124: 2299–309.

Van Paesschen W, Connelly A, King MD, Jackson GD, Duncan JS. The spectrum of hippocampal sclerosis: a quantitative magnetic resonance imaging study. Ann Neurol 1997; 41: 41–51.

Woods RP, Mazziotta JC, Cherry SR. MRI-PET registration with automated algorithm. J Comput Assist Tomogr 1993; 17: 536–46.

Worsley KJ, Evans AC, Marrett S, Neelin P. A three-dimensional statistical analysis for CBF activation studies in human brain. J Cereb Blood Flow Metab 1992; 12: 900–18.

Worsley KJ, Marrett S, Neelin P, Vandal AC, Friston KJ, Evans AC. A unified statistical approach for determining significant signals in images of cerebral activation. Hum Brain Mapp 1996; 4: 58–73.

Received August 5, 2002. Revised December 19, 2002. Accepted January 13, 2003